

PLANETARY ROVER LOCOMOTION ON SOFT GRANULAR SOILS – EFFICIENT ADAPTION OF THE ROLLING BEHAVIOUR OF NONSPHERICAL GRAINS FOR DISCRETE ELEMENT SIMULATIONS

R. LICHTENHELDT¹, B. SCHÄFER¹

¹ German Aerospace Center (DLR)
Robotics and Mechatronics Center
Münchner Strasse 20
D-82234 Wessling
Roy.Lichtenheldt@dlr.de www.dlr.de/rm

Key words: Discrete Element Method, terramechanics, planetary rover, soil interaction, granular soil

Abstract. In consequence of growing interests of science exploration on our solar system's planets and moons, increased mobility demands are arising for planetary exploration vehicles. The locomotion capabilities of these systems strongly depend on the interaction with soft granular soils. Thus a major design challenge is to develop suitable solutions for locomotion equipment and strategies. The mastering of these challenges depends on detailed soil interaction models to predict the system behaviour and get a better understanding of the underlying effects. To meet these demands a new soil interaction model based on the three-dimensional Discrete Element Method (DEM) is developed. The strength of granular materials is highly dependent on the grain's shape and friction. Since non-spherical particles are less computational efficient than spheres, a new interparticle contact model has been developed to mathematically cover the rotational behaviour of anisotropically elongated and angular grains, while using computationally efficient spheres for contact detection. To show the applicability of the model, bevameter as well as single wheel simulations for planetary rovers were carried out.

1 INTRODUCTION

To answer questions about the formation of our solar system and to investigate the existence of extraterrestrial life, the interest in exploration of planetary bodies is increasing consecutively. Hence extended locomotion capabilities are needed for planetary exploration vehicles. Soft granular soils are acting as a limiting factor for mobility and its performance. To further improve the performance of these vehicles, suitable solutions for locomotion equipment and strategies need to be developed. To master this design

challenge, there is a need for detailed soil interaction models to predict the dynamic system behaviour. The usage of such models gives a better understanding of the underlying effects and enables simulation driven development and design.

In addition to empirical models like BEKKER's theory developed back in the 1960's [1], methods like Finite or Discrete Element Method (DEM) became computationally affordable in the field of terramechanics, due to the last years increase of computation power. Thus three-dimensional DEM terramechanics models, currently developed at DLR-RMC, are giving further insights to the soil interaction. These models are based on the DEM simulator tool Pasimodo [2], which is therefore extended by DLR-RMC programmed plugins and wrapped into an external framework.

Nevertheless, it is important to use efficient modeling techniques to gain both high accuracy and affordable computation time. In DEM particle rotations are of major influence on the strength of granular soils. Thereby rotational behaviour is mainly influenced by the grains shape and surface (see [3]). Real soils consist of arbitrarily shaped grains, as they have been subject to extensive wear in the process of their formation. To cover these effects, the use of nonspherical particles results in higher computation efforts for contact detection and possible nonconvex particles. Thus resistance moments or locked particle rotations are commonly used to increase the strength of granular materials. Particles with locked rotation do not cover shear failure due to onsetting particle rotation. Damping torques or rotational velocity scaling strategies [4] could only be applied to dynamic particle flows, as they would not add shear strength in quasi-static and static load cases. In [3], [5], [6] and [7] spherical particles with elastic resistance moments including a plastic torque limitation are used. These resistance moments increase the strength of the granular material, but do not directly correspond to the rolling behaviour of arbitrarily shaped grains. To combine efficient spherical particle geometry and the rotational behaviour of anisotropically elongated and angular grains a new particle contact model has been developed and implemented as a plugin for Pasimodo, by DLR-RMC. Therefore the torques due to tilting motion of the particles are calculated. Because the model mathematically covers the grains rotational behaviour, it is possible to use spheres for contact detection.

2 DISCRETE ELEMENT MODELING

As first announced by Cundall & Strack [8], the discrete element approach features modeling of soft sandy soils on grain scale. Thus the macroscopic soil deformation is based on interparticle contact reactions. By this microscale modeling approach the method implicitly covers the soil's plastic deformation due to grain relocation. The motion states for each particle can be obtained by integration of the principles of linear and angular momentum using the particles contact reaction forces:

$$m\ddot{u}_i = \sum \vec{F}_i^C \quad (1)$$

$$J_i\ddot{\varphi}_i = \sum \vec{M}_i^C \quad (2)$$

whereat \vec{F}_i^C are the contact forces, \vec{M}_i^C are the contact torques and J_i the moment of inertia for each particle. The motion states in translation and rotation are \vec{u}_i and $\vec{\varphi}_i$. To determine these states, Pasimodo's semi-implicit NEWMARK integration scheme is used to achieve larger time steps compared to explicit solvers, as this method is unconditionally stable ([2], [9]).

To map DEM's microscale parameters to the real soil's characteristics the parameter estimation strategy explained in [10] is used. The correspondent translational as well as the newly developed rotational contact modeling approach, based on the mapping of the rotational behaviour of angular grains to computationally efficient spherical particles, will be explained throughout the next sections.

2.1 Translational Contact Reactions

To determine the contact forces, a soft particle approach is used for microscale modeling. Thus the particles are allowed to overlap. The particle's contact forces are partitioned

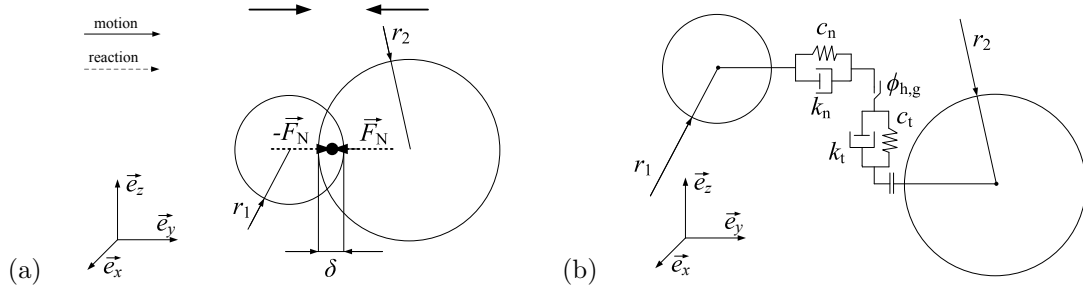


Figure 1: a) Soft particle contact generating overlap and b) contact model for normal and tangential direction

to normal and tangential direction forces. As in Figure 1 the particles overlap δ is used to determine the normal contact reaction force. To restrict the particles overlap, a nonlinear spring-damper element featuring HERTZIAN theory combined with a damping force is applied between the contacting particles m and n :

$$\vec{F}_n^c = \frac{2E}{3(1-\nu^2)} \cdot \sqrt{r_{12} \cdot \delta_{mn}^3} \cdot \vec{n}_c, \quad \forall \delta \neq 0 \quad (3)$$

$$\vec{F}_n^k = \dot{u}_{mn} \cdot k_n \cdot \vec{n}_c \quad (4)$$

$$\vec{F}_N = \vec{F}_n^c + \vec{F}_n^k \quad (5)$$

where E and ν are YOUNG'S modulus and POISSON'S ratio, k_n is the damping coefficient. Furthermore r_{12} is the mean radius and \vec{n}_c is the correspondent contact normal and \dot{u}_{mn} the relative velocity of the contacting particles m and n .

To model the frictional interaction of particles in tangential direction, another spring-damper element is applied between the particles. If the tangential force exceeds the MOHR-

COULOMB yield criterion, the force is restricted to sliding friction by a slider element. Thus the tangential force can be determined as:

$$\vec{F}_t = \begin{cases} c_t \cdot \vec{\delta}_t & \forall \vec{F}_t^c \leq F_N \cdot \tan(\phi_h) \\ \vec{F}_N \cdot \tan(\phi_g) & \forall \vec{F}_t^c > F_N \cdot \tan(\phi_h) \end{cases} \quad (6)$$

whereat \vec{F}_N is the total contact normal force of the particles m and n correspondent to Equations (3) and (4). According Figure 1 $\vec{\delta}_T$ and c_T are the deflection and stiffness of the spring. ϕ_h and ϕ_g are the interparticle stick and slip friction angles. An additional background damping force, which is independent of the current contact situation is used to improve the system stability. k_h is the correspondent damping coefficient.

2.2 Rotational Contact Reactions - Modeling the Grains Shape

The main idea of the model is shown in Figure 2. The angular grains in Figure 2a) are modeled by a rotation geometry and then mapped to the spherical particles for torque calculation (Figure 2b)). For a first implementation of the model rectangular rotation

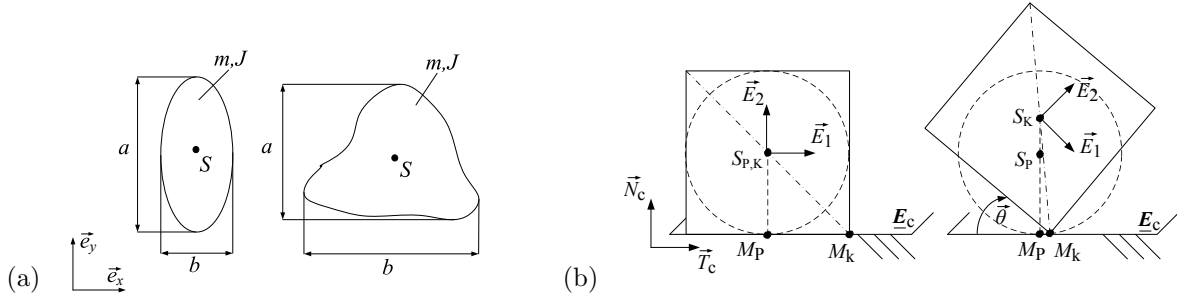


Figure 2: Nonlinear torque law applied to a spherical particle covering the rotational behaviour of angular grains

geometries are used. By applying different rotation geometries for each axis anisotropic rotation behaviour is covered. The rectangular rotation geometries are defined by the aspect ratio angle γ as in Figure 3. The aspect ratio angle γ is defined by the aspect ratio $A = \frac{a}{b}$ as:

$$\gamma = \arctan(A), \quad \gamma \in \left(0; \frac{\pi}{2}\right) \quad (7)$$

where a and b are the geometric dimensions of the grain. Due to the spherical contact detection geometry, the rotation between the particles will take place as the rotation around the sphere's instantaneous center of rotation M_P . Thus the particle's center of mass S_P gains no translational movement (Figure 2) and the virtual rectangle's center of rotation M_K is moved as in Figure 2. Hence as an assumption the sphere is not moved like its virtual rotation geometry representation, but the corresponding torques are

applied. Thus to map the tilting behaviour of arbitrarily shaped grains to computational efficient spheres (Figure 2), the particle's geometry is separated in two parts: (1) The spherical body for contact detection and (2) an additional two dimensional geometrical representation for every rotation in each rotation plane \underline{E}_{jk} (Figure 3b)). Thereby the

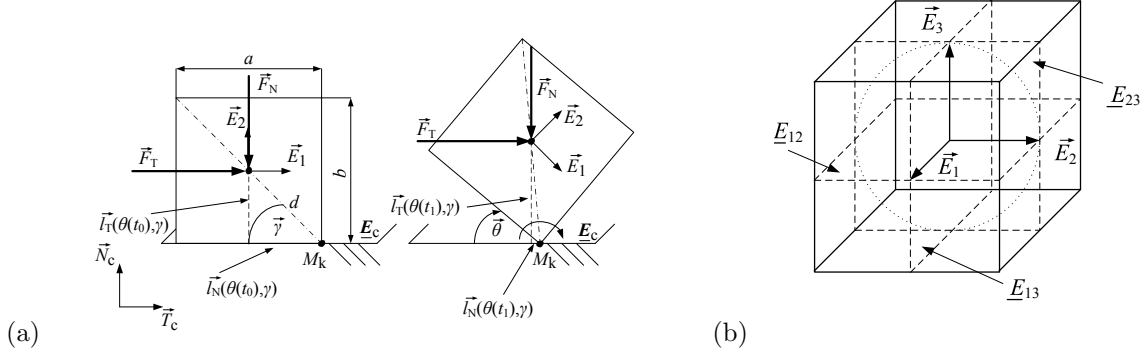


Figure 3: a) Model parameters and b) rotation planes on a spherical and the resulting cubic rotation geometry

local particle coordinate system's basis vectors are the normal vectors of the rotation planes. The particle's local coordinate basis is derived by its rotation quaternion $\bar{q} = [q_0, (q_1, q_2, q_3)]$; $\bar{q} \in \mathbb{H}$ as in [11]:

$$\underline{\mathbf{E}} = \bar{q} \bar{q}' \bar{q}^{-1} \quad (8)$$

$$= (\vec{E}_1 \quad \vec{E}_2 \quad \vec{E}_3) \quad (9)$$

$$= \begin{pmatrix} 1 - 2(q_2^2 + q_3^2) & 2(q_1 q_2 - q_0 q_3) & 2(q_0 q_2 + q_1 q_3) \\ 2(q_1 q_2 + q_0 q_3) & 1 - 2(q_1^2 + q_3^2) & 2(q_2 q_3 - q_0 q_1) \\ 2(q_1 q_3 - q_0 q_2) & 2(q_2 q_3 + q_0 q_1) & 1 - 2(q_1^2 + q_2^2) \end{pmatrix} \quad (10)$$

The force directional vectors \vec{N}_c^{jk} and \vec{T}_c^{jk} for each rotation axis are derived by projecting and normalizing the contact's normal vector \vec{n}_c from global \mathbb{R}^3 to the rotation plane's \mathbb{R}^2 :

$$\vec{N}_c^{jk} = (\vec{n}_c - \langle \vec{n}_c, \vec{E}_i \rangle \cdot \vec{E}_i)_0 \quad i, j, k = [1, 2, 3] \quad i \neq j \neq k \quad (11)$$

$$\vec{T}_c^{jk} = \vec{N}_c^{jk} \times \vec{E}_i \quad (12)$$

thereby \vec{N}_c^{jk} and \vec{T}_c^{jk} are the correspondent normal and tangential force directional vectors in \underline{E}_{jk} . As in Figure 3a) the angle of rotation $\vec{\theta}_i$ around the instantaneous center of rotation M_k is defined as the intersection angle of \vec{E}_j and the contact plane \underline{E}_c . For the projection to the rotation plane's \mathbb{R}^2 and $\vec{T}_c^{jk} \in (\underline{E}_c, \underline{E}_{jk})$, $\vec{\theta}_i$ is derived by the intersection of \vec{T}_c^{jk} and \vec{E}_j . The torques are caused by tangential as well as normal forces (Figure 3). In order

to calculate the resultant Force \vec{F}_R^{jk} , the total contact forces \vec{F}_c , which is calculated from the translational contact reactions, need to be projected to the rotation plane:

$$\vec{F}_R^{jk} = \vec{F}_c - \langle \vec{F}_c, \vec{E}_i \rangle \cdot \vec{E}_i \quad i, j, k = [1, 2, 3] \quad i \neq j \neq k \quad (13)$$

Using these forces the torque \vec{M}_P is derived using the moment arms l_N^{jk} and l_T^{jk} :

$$\begin{aligned} \vec{M}_P = \sum_{i,j,k=1}^3 \left(\vec{F}_R^{jk} \times \left[l_T^{jk}(\theta_i(t), \gamma_i) \cdot \vec{N}_c^{jk} \right] + \right. \\ \left. \vec{F}_R^{jk} \times \left[l_N^{jk}(\theta_i(t), \gamma_i) \cdot \vec{T}_c^{jk} \right] \right) \\ i, j, k = [1, 2, 3] \wedge i \neq j \neq k \end{aligned} \quad (14)$$

As in Figure 3b) the effective length of the moment arms is dependent on the aspect ratio and the current rotation angle θ . Figure 4 shows this dependency for different aspect ratios A . These nonlinear dependencies are covered analytically in the model.

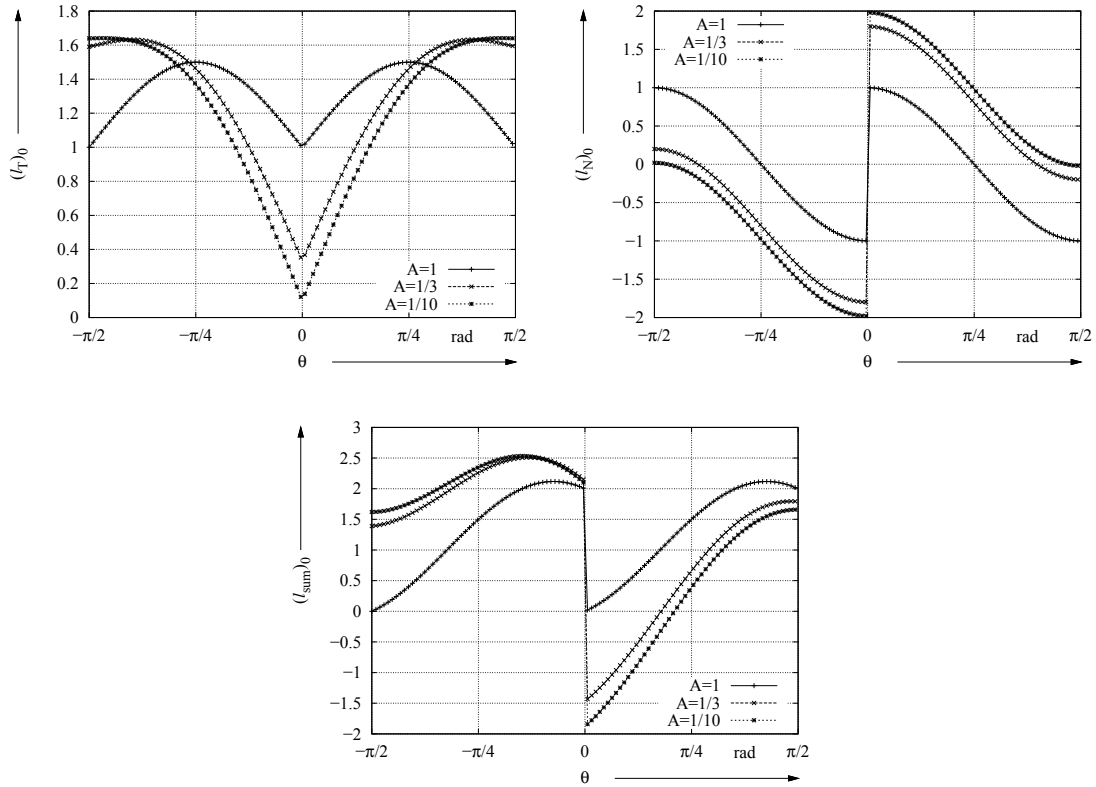


Figure 4: Effective length of the moment arms in nonlinear dependency of the tilting angle: tangential arm l_T (upper left), normal arm l_N (upper right) and resulting arm l_{sum} (bottom)

The torque due to l_N is causing the resistance against tilting, until the tilting angle is met and its sign changes the torque to a propulsive one as well. This tilting angle is influenced by the aspect ratio angle γ . The moment arm l_T is causing only propulsive torques and l_{sum} is the summed moment arm. An additional smoothing function could be applied if needed for stability issues. The particle's moment of inertia J_i is adapted to the new rotation geometry by combining the sphere's mass and the moment of inertia for a thin rod. It is calculated based on the material density ρ , the particle's radius r and the aspect ratio:

$$J_i = \frac{1}{9} \cdot \pi \rho r^3 \left(\frac{r}{A_i} \right)^2 \quad (15)$$

Figure 5 gives some examples of the possible shapes that can be modeled by this approach. To model geometries like the rectangular bar an additional scaling factor s_i is introduced for every rotation geometry. Aspect ratios $A \leq 1$ are chosen, as their rotation geometry is then limited by r . For equal aspect ratio in two axis and free rotation in the third, it is possible to model cylindrical shapes like in Figure 5c).

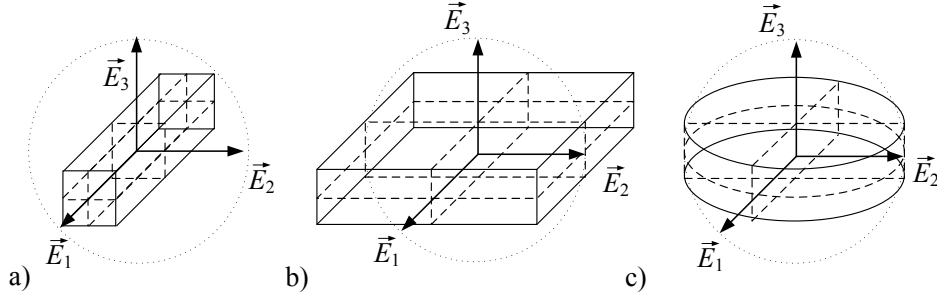


Figure 5: Examples for resulting rotation geometries: a) rectangular bar b) rectangular plate c) cylindrical disc

Table 1 shows how the parameters of the model need to be chosen to resample the shapes shown in Figure 5. Additionally the parameters for cubic representations are given, which are shown in Figure 3b).

Parameter	cube	bar	plate	cylindrical disc
A_1	1	1	$< A_3$	< 1
A_2	A_1	$< A_1$	A_1	< 1
A_3	A_1	A_2	1	–
s_1	1	A_2	1	1
s_2	1	1	1	1
s_3	1	1	1	–

Table 1: Paramaters to build sample shapes as in Figure 5

3 SIMULATION RESULTS

3.1 Bevameter Simulations

To show the models capabilities bevameter (see also [12]) tests are simulated. The bevameter is commonly used to measure the soil's mechanical parameters and strength in the field of terramechanics. In Figure 6 the model setup is shown. For the test a cylindrical plate is pressed into the soil with a defined velocity, while the pressure on the plate and the current sinkage are measured. Therefore information on the soils load bearing capacity can be retrieved from the tests. A first verification for the bevameter simulations for milled lava soil RMC-Soil03 is shown in [10]. First parametric simulation studies have

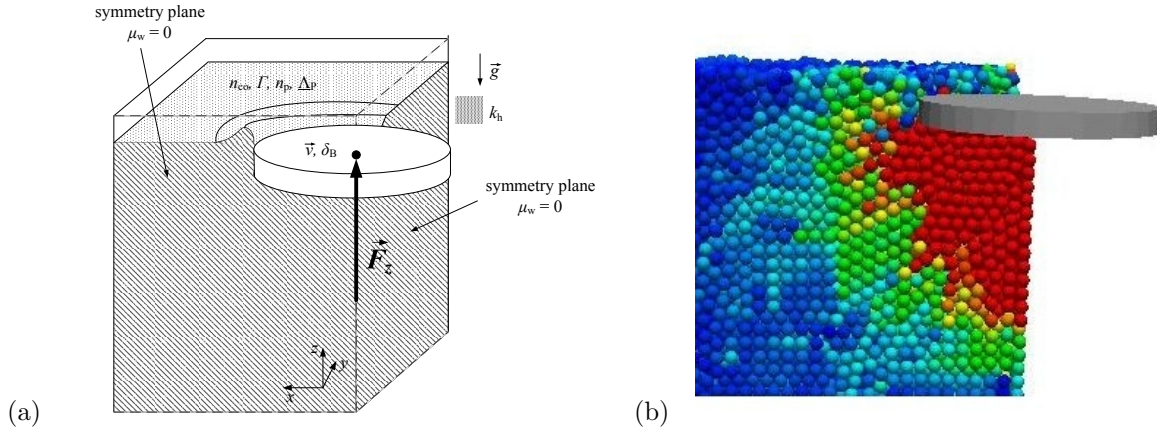


Figure 6: a) Bevameter model setup and b) bevameter simulation in Pasimodo

been carried out dependent on the interparticle friction and the aspect ratio, as they are assumed to be the main influencing parameters for the shear strength. Figure 7 a) shows the pressure-sinkage relation dependent on the aspect ratio. For these simulations a high interparticle friction angle of $\phi = 55^\circ$ is chosen to investigate the rolling behaviour. It can be seen that for lower sinkage the pressure for the different aspect ratios is nearly the same as the pressure for fixed rotation particles. For higher sinkage the smaller aspect ratios tend to show minor increase of pressure over sinkage. It is assumed that this is caused by onsetting particle rotation due to lower rotation resistance. As it can be seen in Figure 4, aspect ratios $A \neq 1$ feature asymmetric total moment arm dependencies and therefore torque characteristics. This fact leads to higher mean rotational velocities of the particles, as they are to tilt easier if resting on the shorter side. Values of $A \geq 1$ are causing higher pressure per sinkage than the lower values. Additionally the scaling parameters s_i could be used to further tune the model towards free rotation. Figure 7b) shows the dependency of the pressure-sinkage relation on the interparticle friction angle for an aspect ratio of $A = \frac{1}{10}$. In addition this dependency is shown for particles using free (pure spherical) and fixed rotation in Figure 8. As there is a big

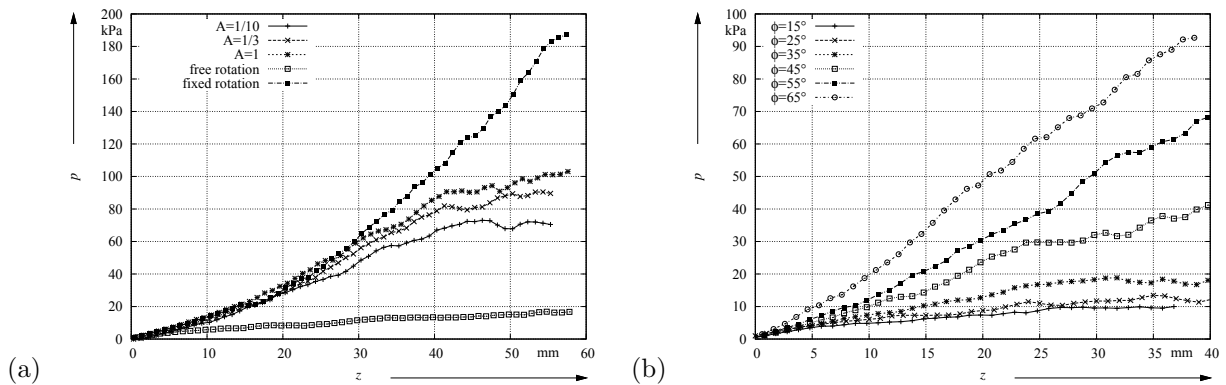


Figure 7: a) Bevameter pressure-sinkage relation dependent on the aspect ratio (left) and b) for $A = \frac{1}{10}$ dependent on the interparticle friction angle (right)

difference in the pressure development between free and fixed rotation especially for high friction values, Figure 7 shows the ability of the model to close that gap by covering the rotational behaviour of angular grains.

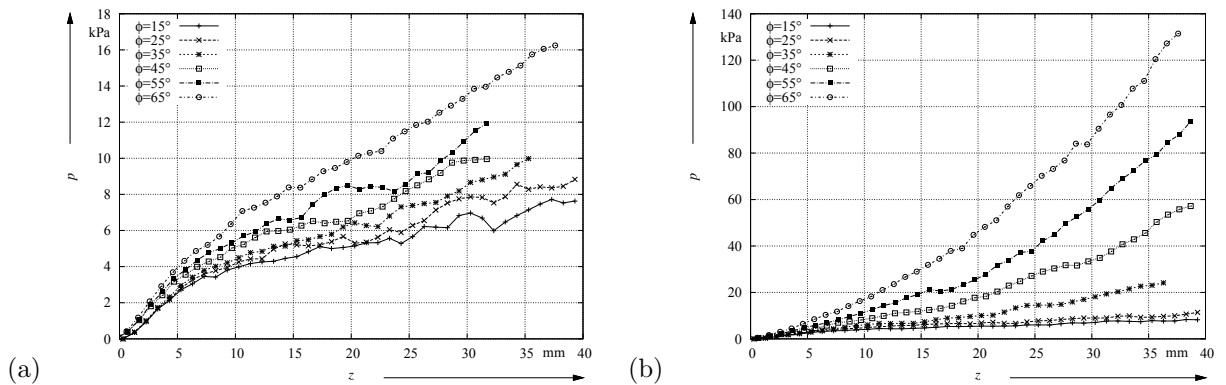


Figure 8: Bevameter pressure-sinkage relation dependent on the interparticle friction angle for a) free (left) and b) fixed rotation (right)

3.2 Application to Wheeled Rover Locomotion

Soft granular soils are a particular challenge for wheeled exploration vehicles, as they are causing high sinkage and motion resistance. As a worst case the whole rover could get stuck like one of NASA's MER rovers. To lower these risks and to improve the locomotion performance of the vehicle, DEM simulations are applied to planetary rover wheels. The DEM model for single wheel simulation consists of a particle filled soil bin and the wheel's representation. The boundaries as well as the wheels are represented by triangulated surfaces. The wheel surface (as in Figure 9b)) is created by parametric equations and imported to Pasimodo, where it is used as one fully dynamic compound.

Mirror symmetry as well as systematic scaling of the particle size are used to reduce computation time (as in [10]). The proposed model has been applied to simulations of an Exomars sized wheel ($d_{\text{wheel}} = 250 \text{ mm}$, $m_{0,5} = 8,33 \text{ kg}$, 12 grousers). The formation of bumps in front and to the side of the wheel, as well as transported particles on the inner wheel surface were discovered in both simulation and tests as shown in Figure 9. Particles trapped inside the grousers are caused by the open wheel surface model. A single wheel testbed which is under current development will be used for further validation of the model. To evaluate the effect of the proposed model, another set of simulations has been

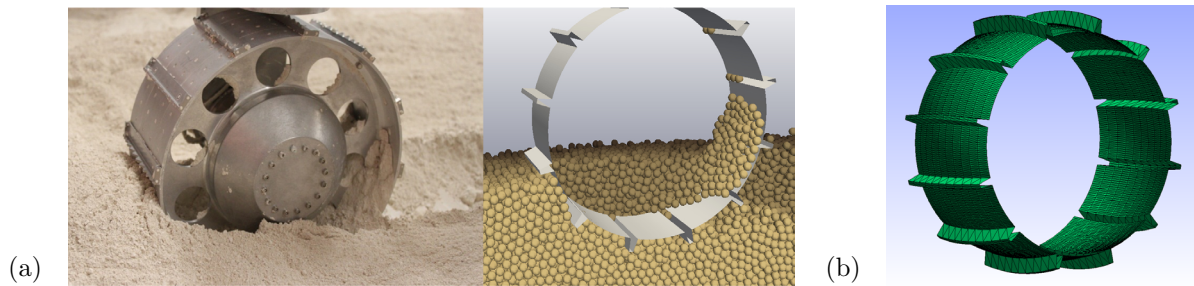


Figure 9: a) Comparison of the rover's wheel (left) and the simulated wheel (right) traveling through the soil and b) Example for triangulated wheel surface

carried out. To compare the tilting model to particles with free rotation for the Exomars sized wheel, lower interparticle friction, thus softer soil, has been used. For the tilting model an aspect ratio of $A = 0.5$ is used and all other parameters are held constant. The results for static as well as dynamic sinkage with respect to the traveled distance are shown in Figure 10. Minor static as well as dynamic sinkage have been observed for

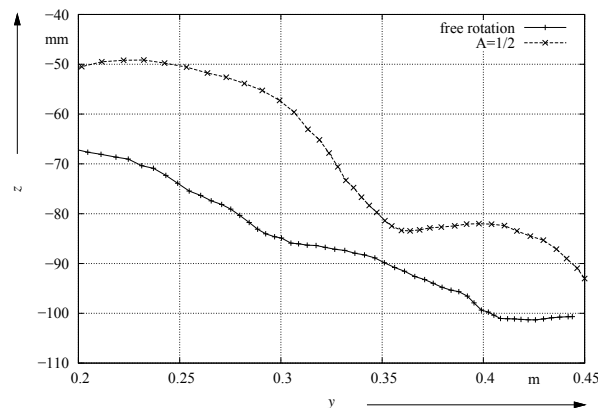


Figure 10: Sinkage development for free and tilting rotation

the tilting model, which is due to the increased soil strength. Furthermore for the tilting model a decreased mean slip of 67% has been observed in comparison to 81% for free rotation.

3.3 Further Application - Hammering beneath the Surface of Mars

Other than for rover wheels, for the DLR developed HP³-Mole (Heat Flow and Physical Properties Package), a payload supplied by DLR to NASA's InSight Mission, hard soils are the worst case condition. As its aim is to hammer itself below the planetary surface of Mars, the mole has to overcome the soil strength with every stroke. First studies using two dimensional Discrete Element modeling (Figure 11) proved the applicability of the model for this kind of locomotion. Effects like lower stroke performance with increasing total penetration depth due to higher soil compaction were covered. Furthermore regarding worst case hard soils without the need of fixed rotation is improving the models accuracy. To model and optimize the internal hammering mechanism, a multibody approach regarding the internal contact dynamics is used. To get a deeper understanding of mechanism's complex behaviour, a one dimensional empirical soil model is currently used. As the outer forces caused by the soil are influencing the dynamics of the internal hammering mechanism, a connection of multibody and DEM model will be carried out. This ongoing co-simulation approach will then be used to analyse influences of the outer shape of the mole as well as to apply further performance optimization.

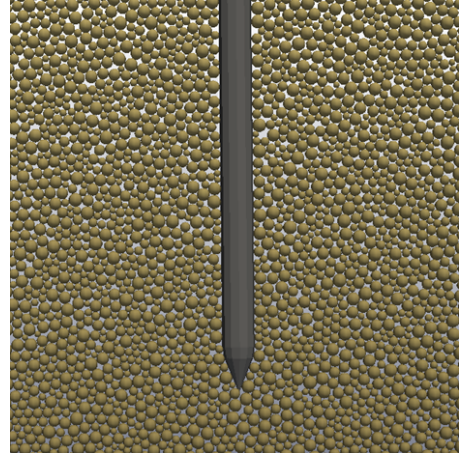


Figure 11: Two dimensional DEM model of the HP³-Mole

4 CONCLUSION

Efficient state of the art rotational contact models are restricted to the application of rolling resistance, without taking the tilting behaviour of angular grains into account. The presented contact model mathematically covers this behaviour and thus naturally features rolling resistance due to tilting motion. Therefore it is capable of covering shear failure due to onsetting particle rotation, while using only the aspect ratio A as one additional parameter. As the model shows only slightly higher computational effort, it is supposed to be applied to simulations, where both efficiency as well as detailed coverage of the particles interaction are needed.

Beviameter simulations have been used to analyze and evaluate the models capabilities. In these simulations the proposed increase of soil strength has been proven and the model has been compared to particles with fixed and free rotation. The model has been applied to two kinds of locomotion for planetary exploration. For rover wheels decreased slip and sinkage were observed using the proposed model compared to free rotational spheres. For the second type of locomotion applications, the hammering into planetary surfaces, a first approach of a two dimensional DEM model has been shown. This model will be used further for co-simulations and thus further analysis and optimization.

References

- [1] Bekker, M.G., Introduction to Terrain - Vehicle Systems, University of Michigan Press, Ann Arbor, 1969
- [2] Fleissner, F., Pasimodo v1.9.3, software package and template files, Inpartik & ITM University of Stuttgart, Tübingen, 2012
- [3] Oda, M.; Iwashita, K., Study on couple stress and shear band development in granular media based on numerical simulation analyses, International Journal of Engineering Science, 2000
- [4] Wu, W., Modellierung von Massenbewegungen: Stand der Technik und neue Entwicklungen, Institut für Geotechnik, Universität für Bodenkultur, Wien, 2010
- [5] Rojek, J.; Zarate, F.; Agelet de Saracibar, C.; Gilbourne, C.; Verdot, P., Discrete element modelling and simulation of sand mould manufacture for the lost foam process, International Journal for Numerical Methods in Engineering, 2005
- [6] Plassiard, J.-P.; Belheine, N.; Donze, F.-V., Calibration procedure for spherical discrete elements using a local moment law, University Grenoble, 2007
- [7] Kozicki, J.; Tejchman, J., Numerical simulations of sand behaviour using DEM with two different descriptions of grain roughness, 2. International Conference on Particle-based Methods- Fundamentals and Applications, 2011
- [8] Cundall, P. A.; Strack, O. D. L., A discrete numerical model for granular assemblies, Geotechnique, 1979, 29, 47-65
- [9] Willner, K., Kontinuums- und Kontaktmechanik, Springer-Verlag, Berlin, 2003
- [10] Lichtenheldt, R.; Schäfer, B., Locomotion on soft granular Soils: A Discrete Element based Approach for Simulations in Planetary Exploration, 12th Symposium on Advanced Space Technologies in Robotics and Automation, ESA/ESTEC, Netherlands, 2013
- [11] DeLoura, M.A., Game Programming: Gems, Band 1, Charles River Media Inc., Hingham, 2000
- [12] Wong, J.Y., Terramechanics and Off-Road Vehicle Engineering, Elsevier Ltd., Amsterdam, 2010